JAES | JOURNAL OF APPLIED ENGINEERING SCIENCE | www.engineeringscience.rs
ISTRAŽIVANJA I PROJEKTOVANJA ZA PRIVREDU

Indexed by

STABILITY OF TANKER TRUCKS USING THE DAVIES METHOD

Gonzalo Guillermo Moreno Contreras
Department of Mechanical, Mechatronic and Industrial Engineering, Faculty of Engineering, University of Pamplona, Pamplona, 543050, Colombia

Elkin Flórez Serrano
Department of Mechanical, Mechatronic and Industrial Engineering, Faculty of Engineering, University of Pamplona, Pamplona, 543050, Colombia

Bladimir Ramón
Department of Mechanical, Mechatronic and Industrial Engineering, Faculty of Engineering, University of Pamplona, Pamplona, 543050, Colombia

Key words: *tanker trucks, stability, rollover, Davies method*
doi:10.5937/jaes0-33364

Cite article:

Guillermo Moreno Contreras G., Flórez Serrano E., Ramón B. (2022) STABILITY OF TANKER TRUCKS USING THE DAVIES METHOD, *Journal of Applied Engineering Science*, 20(2), 602 - 609, DOI:10.5937/ jaes0-33364

Online aceess *of full paper is available at: www.engineeringscience.rs/browse-issues*

doi:10.5937/jaes0-33364

Paper number: 20(2022)2, 967, 602-609

STABILITY OF TANKER TRUCKS USING THE DAVIES METHOD

Gonzalo Guillermo Moreno Contreras*, Elkin Flórez Serrano, Bladimir Ramón
Department of Mechanical, Mechatronic and Industrial Engineering, Faculty of Engineering, University of Pamplona, Pamplona, 543050, Colombia

The stability of heavy vehicles is an issue that has been worked on in recent times. For this, several models that allow to determine how prone a vehicle is to rollover have been developed. However, most of these models use fixed loads to take their measurements without including shifting loads that in certain cases decrease the stability of the vehicles. With this in mind, this article proposes a two-dimensional kinematic model to determine the Static Rollover Threshold (SRT) using the Davies Method as an analysis tool. Lastly, a case study is carried out to determine the influence of the load on the reduction of vehicle stability.

Key words: tanker trucks, stability, rollover, Davies method

INTRODUCTION

The transport of liquid cargo is often dangerous since due to its movement, the load distribution on the vehicle easily shifts, causing cases serious accidents in some cases. It is because of this that different shapes and tank configurations are used to transport liquids. Taking the aforementioned into account, one of the main causes of accidents for these vehicles are rollovers when they take a curve, which causes the inertial force of the load to act a way that makes the vehicle lose balance and overturn. Authors such as [1] and [4] have developed models to determine how the tank's filling percentage and the movement of the transported fluid can affect vehicle stability. Other authors such as [5], [6] have calculated the stability of these vehicles using the Tilt Table test. However, in the present model all these aspects are integrated using the model developed by [7], in which the Davies method [8], [9] is used. This technique allows calculating the kinetics of the mechanism taking into account several vehicle characteristics. Therefore, this paper presents the implementation of a kinematic model to determine the Static Rollover Threshold (SRT) using the Davies method (Chapters 2 and 3), followed by a case study. The results of this factor's calculation will be presented in detail. Finally, the conclusions of this study are shared.

MOVEMENT OF FLUID WITH UNIFORM ACCELERATION

The equations that describe the linear movement of an incompressible fluid inside a circular tank subjected to uniform acceleration (Fig. 1) are the continuity equations and the momentum conservation equation [10], which is presented in the Eqs.1 and 2

$$\nabla \cdot v = 0 \tag{1}$$

and

$$\rho\left(\frac{\partial v}{\partial t} + v \cdot \nabla v\right) = -\nabla P + \rho g + \mu \nabla^2 v \tag{2}$$

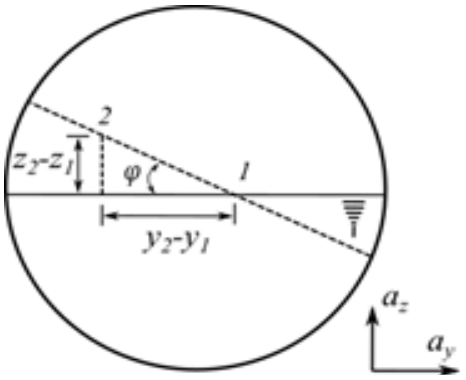

Figure 1: Fluid in acceleration in tank of circular cross-section

Where u is the fluid velocity [m/s], P is the fluid pressure [Pa], ρ is the fluid density [kg/m3], μ is the viscosity of the fluid [Pa.s], and g is the acceleration due to gravity [m/s^2]. When the fluid is subjected to lateral acceleration, each element of the fluid in the tank experiences the same acceleration, also, its velocity v is a function of time but not of position, Eq.2 can be rewritten as:

$$\rho \frac{Dv}{Dt} = -\nabla P + \rho g + \mu \nabla^2 v \tag{3}$$

Where D/D_t is the substantial derivative for a uniformly accelerated flow, Du/Dt = a and $\nabla^2 v$ which reduces Eq.3 to:

$$\rho a = -\nabla P + \rho g \tag{4}$$

Equation 4 can be expressed as:

$$\frac{\partial P}{\partial x}\vec{i} + \frac{\partial P}{\partial y}\vec{j} + \frac{\partial P}{\partial z}\vec{k} + \rho g\vec{k} = -\rho\left(a_x\vec{i} + a_y\vec{j} + a_z\vec{k}\right) \tag{5}$$

**gmoren@unipamplona.edu.co*

Considering the movement of the fluid in the y-z plane, Eq.5 is reduced to:

$$dP = -\rho a_y dy - \rho(g + a_z)dz \tag{6}$$

When a tank is uniformly accelerated in the y-direction, the free surface will move back and forth initially; after some time this movement disappears, going from this transient state into a uniformly accelerated movement. The position of the liquid surface in a uniformly accelerated tank is shown in Fig.1. For ρ = constant, the pressure difference between two points 1 and 2 in the fluid is determined by integration, so that the Eq. 6 becomes:

$$P_2 - P_1 = -\rho a_y(y_2 - y_1) - \rho(g + a_z)(z_2 - z_1) \tag{7}$$

The vertical increase of the free surface at point 2 relative to point 1 can be determined by selecting these points on the free surface where P2 = P1 and solving Eq.7.

$$\Delta z = z_2 - z_1 = -\frac{a_y}{g + a_z}(y_2 - y_1) \tag{8}$$

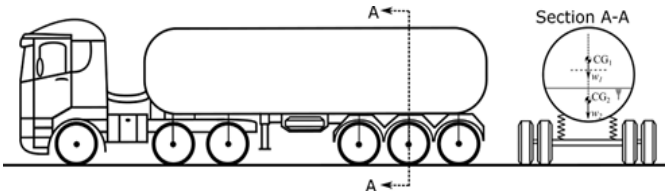

Figure 2: Road Tanker

Initially, when the vehicle takes a curved trajectory (in this case to the right) it can be observed that the centripetal inertial forces (m1ay and m2ay) are in their respective centers of gravity (Fig. 3), these forces make the vehicle, influenced by the action of stiffness of the tires and the load put in its suspension system, tilts in a θ angle, which causes the movement of the CG1 around the vehicle's center of rotation (CR), then, the transported liquid assumes its new horizontal position, which makes that the CG2 move toward its initial position, moving similarly to a pendulum around the tank's geometric center. In an incompressible fluid with uniform acceleration in linear motion, the lines of constant pressure are parallel to the surface, the slope in the y - z plane with az = 0 can be determined by

$$\text{slope} = -\frac{a_y}{g + a_z} = -\frac{a_y}{g} = \tan\varphi \tag{9}$$

In order to determine the fluid's center of gravity (CG2) in a circular cross-section tank subject to uniform acceleration and with a certain filling percentage , the center of gravity's coordinates are determined by solving:

$$\bar{x} = \frac{1}{A}\iint_A x dA \tag{10}$$

$$\bar{y} = \frac{1}{A}\iint_A y dA \tag{11}$$

VEHICLE STABILITY ANALYSIS

For this analysis, the two-dimensional representation of the tanker truck with a circular cross-section was used (Fig. 2 - Section AA), in it. it can be appreciated that the vehicle has a fixed center of gravity (CG1), which corresponds to the non-mobile weight of the vehicle (w1), and a moving center of gravity (CG2), which represents the transported fluid's weight (w2), it is assumed by what is specified in section 2, that the fluid's movement is linear. In order to be able to observe the fixed vehicle's weight movement (CG1), a large height was used for the figures.

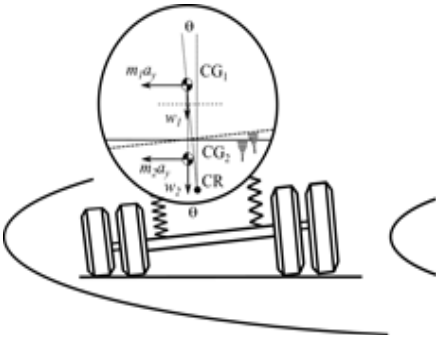

Figure 3: Tanker truck under the inclination angle action (θ)

Additionally, due to the fluid's linear movement as a result of its lateral acceleration, the mobile load's center of gravity (CG2) moves in a greater angle (θ_1), first due to vehicle inclination (Fig. 3) and second due to the transported fluid's movement.

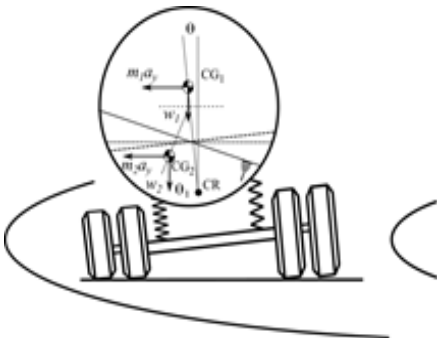

Figure 4: Tanker truck under the action of the transported fluid's movement

Taking into account the center of gravity movement specifications, it is possible to carry out that described by [7], where the two-dimensional model of the vehicle (Fig.5 (a)) is represented by a kinematic model (Fig.5 (b)). Once the model is made and using the Davies Method as an analysis tool [11] and [13], it is possible

to obtain the vehicle stability factor (SRT) and the forces acting in each of the developed model's systems (suspension and tires).

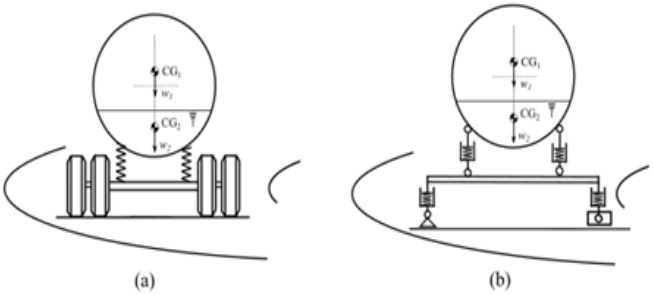

Figure 5: (a) Two-dimensional model of the vehicle. (b) Kinematic model of the vehicle

For the implementation of the Davies method, it is important to list the joints and links, according to Fig 6, the numbers indicate the joints (1, 4, 6, 8, 9 and 11 are rotary joints on the X-axis, 3 is a prismatic joint on the Y-axis and joints 2, 5, 7 and 10 are prismatic joints on the Z-axis) and the letters are the mechanism links (A - the ground, B - the left tire, C-D the right tire, E - axle, F-G and H-I suspension, and J is the tank).

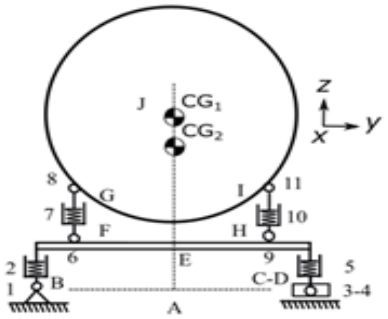

Figure 6: Kinematic model of the vehicle

Screw Theory

This theory is divided into two parts, the first is the successive screw displacement method to determine the mechanism's joints immediate position each time it moves, and the second is that which allows us to determine the representation the forces and momentum that acts on each joint.

Successive screw displacement method

As mentioned above, it is possible to determine the immediate position of each of the reference points that make up the mechanism through this technique [13]. In Fig. 7 and Table 1 the screw parameters are indicated, where s is the unit vector along the direction of the screw axis (Fig. 7a), s_0 is the position vector of a point lying along the screw axis, θ_i is the rotation angle of the joint or the screw and d_i is the translation of the joint or the screw.

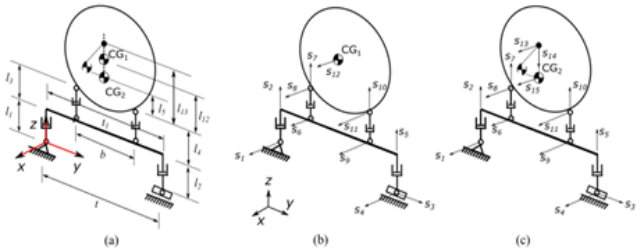

Figure 7: Variables of the mechanism position. a) Position vector (s_0). b) and c) Screw axis direction vector (s)

In Fig. 7 and Table 1: $l_{1,2}$ are the dynamic radii of the tires, $l_{3,4}$ are the suspension height, l_{12} is the height of the CG_1 above the chassis, l_{13} is the height of the rotation point of CG_2, l_5 is the height of the CG_2 above the chassis, t is the track widths, t_1 is the axle widths, and b is the lateral separation between the suspension's leaf springs .The screw parameters allow determining the rotation matrices (A_i) and the position matrix (p_i) for each joint with which it is possible to determine the immediate position of each joint or reference point by applying the successive screw displacement method, which is indicated in Table 2 (s_{oi}).

Wrench

According to [9], [11] the forces and momentum present in the mechanism are represented by wrenches, according to Eqs. 12 and 13, respectively

$$\$^A = \begin{Bmatrix} s_{0i} \times s_i \\ s_i \end{Bmatrix} F_i \tag{12}$$

$$\$^A = \begin{Bmatrix} s_i \\ 0 \end{Bmatrix} M_i \tag{13}$$

Where F_i is the constraint force applied on the joint i, s_{0i} is the immediate position vector for reference point i (Table 3), s_i is the wrench orientation vector, and M_i is the constraint moment applied to the joint i. The wrench can be represented in a more compact form, according to Eq. 14.

$$\$^A = \hat{\$}^A \Psi \tag{14}$$

Where $\hat{\$}^A$ is the normalized wrench and Ψ is its magnitude.

- For the proposed model, the following considerations were made:
- For the x-direction, a steady-state model was used in the analysis,
- Road deformations and lateral friction in joint 3 was neglected,
- The only forces acting in the model are the weights (w1 and w2) and the inertial forces (m_1a_y and m_2a_y).

Table 1: Screw parameters of the mechanism

Joint or reference point	s			s_0			θ	d
	s_x	s_y	s_z	s_{0x}	s_{0y}	s_{0z}		
Joint 1	1	0	0	0	0	0	θ_1	0
Joint 2	0	0	1	0	0	0	0	l_1
Joint 3	0	1	0	0	0	0	0	t
Joint 4	1	0	0	0	0	0	θ_4	0
Joint 5	0	0	1	0	0	0	0	l_2
Joint 6	1	0	0	0	$\frac{t_1-b}{2}$	0	θ_6	0
Joint 7	0	0	1	0	$\frac{t_1-b}{2}$	0	0	l_3
Joint 8	1	0	0	0	$\frac{t_1-b}{2}$	0	θ_8	0
Joint 9	1	0	0	0	$\frac{t_1+b}{2}$	0	θ_9	0
Joint 10	0	0	1	0	$\frac{t_1+b}{2}$	0	0	l_4
Joint 11	1	0	0	0	$\frac{t_1+b}{2}$	0	θ_{11}	0
Joint 12 (CG_1)	1	0	0	0	$\frac{t_1}{2}$	l_{12}	0	0
Joint 13 (Construction CG_2)	1	0	0	0	$\frac{t_1}{2}$	l_{13}	θ_{13}	0
Joint 14 (Construction CG_2)	0	0	-1	0	$\frac{t_1}{2}$	l_{13}	0	l_5
Joint 15 (CG_2)	1	0	0	0	$\frac{t_1}{2}$	l_{13}	0	0

Table 2: Instantaneous position vector (s_{0i})

Joint or reference point	s_{0i}		
	s_{0ix}	s_{0iy}	s_{0iz}
Joint 1	0	0	0
Joint 2	0	$-l_1 \sin(\theta_1)$	$l_1 \cos(\theta_1)$
Joint 3 y 4	0	t	0
Joint 5	0	$t - l_2 \sin(\theta_4)$	$l_2 \cos(\theta_4)$
Joint 6	0	$-l_1 \sin(\theta_1) + \left(\frac{t_1-b}{2}\right)\cos(\theta_1)$	$l_1 \cos(\theta_1) + \left(\frac{t_1-b}{2}\right)\sin(\theta_1)$
Joint 7 y 8	0	$-l_1 \sin(\theta_1) + \left(\frac{t_1-b}{2}\right)\cos(\theta_1) - l_3 \sin(\theta_1+\theta_6)$	$l_1 \cos(\theta_1) + \left(\frac{t_1-b}{2}\right)\sin(\theta_1) + l_3 \cos(\theta_1+\theta_6)$
Joint 9	0	$-l_1 \sin(\theta_1) + \left(\frac{t_1+b}{2}\right)\cos(\theta_1)$	$l_1 \cos(\theta_1) + \left(\frac{t_1+b}{2}\right)\sin(\theta_1)$
Joint 10 y 11	0	$-l_1 \sin(\theta_1) + \left(\frac{t_1+b}{2}\right)\cos(\theta_1) - l_4 \sin(\theta_1+\theta_9)$	$l_1 \cos(\theta_1) + \left(\frac{t_1+b}{2}\right)\sin(\theta_1) + l_4 \cos(\theta_1+\theta_9)$
Joint 12 (CG_1)	0	tb_1	h_1
Joint 15 (CG_2)	0	tb_2	h_2

Where: $tb_1 = -l_1 \sin(\theta_1) + \left(\frac{t_1 - b}{2}\right)\cos(\theta_1) - l_3 \sin(\theta_1 + \theta_6) - l_{12} \sin(\theta_1 + \theta_6 + \theta_8) + \frac{b}{2}\cos(\theta_1 + \theta_6 + \theta_8)$

$$h_1 = l_1 \cos(\theta_1) + \left(\frac{t_1 - b}{2}\right)\sin(\theta_1) + l_3 \cos(\theta_1 + \theta_6) + l_{12} \cos(\theta_1 + \theta_6 + \theta_8) + \frac{b}{2}\sin(\theta_1 + \theta_6 + \theta_8)$$

$$tb_2 = -l_1 \sin(\theta_1) + \left(\frac{t_1 - b}{2}\right)\cos(\theta_1) - l_3 \sin(\theta_1 + \theta_6) - l_{13} \sin(\theta_1 + \theta_6 + \theta_8) + \frac{b}{2}\cos(\theta_1 + \theta_6 + \theta_8) - l_5 \sin(\theta_1 + \theta_6 + \theta_8 + \theta_{13})$$

$$h_2 = l_1 \cos(\theta_1) + \left(\frac{t_1 - b}{2}\right)\sin(\theta_1) + l_3 \cos(\theta_1 + \theta_6) + l_{13} \cos(\theta_1 + \theta_6 + \theta_8) + \frac{b}{2}\sin(\theta_1 + \theta_6 + \theta_8) - l_5 \cos(\theta_1 + \theta_6 + \theta_8 + \theta_{13})$$

Table 3: Wrench parameters of the mechanism

Joint or reference point	Constraints and forces	s_i			Immediate position vector s_{0i} (Table 2)
		s_{ix}	s_{iy}	s_{iz}	
Revolute joints 1, 4, 8, 9 y 11	F_{yi}	0	1	0	Revolute joints 1, 4, 8, 9 y 11 respectively
	F_{zi}	0	0	1	
Prismatic joint 3	M_{xi}	1	0	0	Prismatic joint 3
	F_{zi}	0	0	1	
Revolute joint 6	T_{xi}	1	0	0	Revolute joint 6
	F_{yi}	0	1	0	
	F_{zi}	0	0	1	
Prismatic joints 2, 5, 7 y 10	M_{xi}	1	0	0	Prismatic joints 2, 5, 7 y 10
	F_{pi}	0	$\cos\theta_{i-1}$	$\sin\theta_{i-1}$	
Prismatic joints 2 y 5	F_{Ti}	0	$-\sin\theta_{i-1}$	$\cos\theta_{i-1}$	Prismatic joints 2 y 5
Prismatic joints 7 y 10	F_{LSi}	0	$-\sin\theta_{i-1}$	$\cos\theta_{i-1}$	Prismatic joints 7 y 10
CG_1	$m_1 a_y$	0	-1	0	CG_1
	w1	0	0	-1	
CG_2	$m_2 a_y$	0	-1	0	CG_2
	w_2	0	0	-1	

All of the wrenches comprise the action matrix [A_d], which are represented in their normalized form according to the Eqs. 15 and 16.

$$[\hat{A}_d]_{3\times 31} = \begin{bmatrix} 0 & 0 & -l_1 & \cdots & h_1 & tb_1 & h_2 & tb_2 \\ 1 & 0 & c1 & \cdots & -1 & 0 & -1 & 0 \\ 0 & 1 & s1 & \cdots & 0 & -1 & 0 & -1 \end{bmatrix} \quad (15)$$

$$[\Psi]_{1\times 31} = [F_{y1} \quad F_{z1} \quad F_{p2} \quad \cdots \quad m_1 a_y \quad w_1 \quad m_2 a_y \quad w_2] \quad (16)$$

Where c1 = $\cos\theta_1$ and s1 = $\sin\theta_1$.

Graph theory

The vehicle's kinematic model (Fig. 6) can be represented in a more abstract approach by a graph (Fig. 8), this graph is composed by ten vertices (links) and 15 edges (joints and external forces).This graph can be explained using an incidence matrix I[10 x 15] (Eq. 17), solving this equation using the Gauss-Jordan method, the cut-set matrix is obtained Q[9 x 15] (Eq. 18), which are indicated by the equation's rows . Additionally, the rearranged cut-set matrix (Eq. 18) can determined the branches (edges 1, 2, 3, 4, 6, 7, 8, 9 y 10) and the chords (edges 5, 11 and the external forces), as shown in Eq. 20, and Fig. 9a, additionally, in Fig. 9b is the mechanism's cut-set action graph is presented.

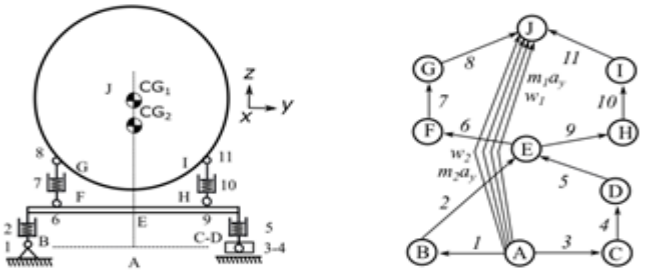

Figure 8: Mechanism and direct mechanism's coupling graph

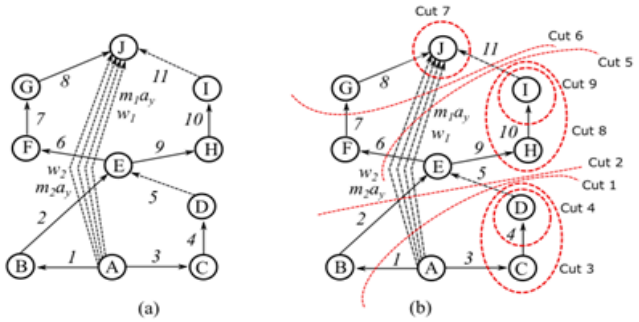

Figure 9: a) Graph with branches and chords. b) Mechanism's cut-set action graph

$$I_{[10x15]} = \begin{array}{c} \\ A \\ B \\ C \\ D \\ E \\ F \\ G \\ H \\ I \\ J \end{array} \begin{array}{c} \begin{array}{ccccccccccccccc} 1 & 2 & 3 & 4 & 5 & 6 & 7 & 8 & 9 & 10 & 11 & m_1a_y & w_1 & m_2a_y & w_2 \end{array} \\ \begin{bmatrix} 1 & 0 & 1 & 0 & 0 & 0 & 0 & 0 & 0 & 0 & 0 & 1 & 1 & 1 & 1 \\ -1 & 1 & 0 & 0 & 0 & 0 & 0 & 0 & 0 & 0 & 0 & 0 & 0 & 0 & 0 \\ 0 & 0 & -1 & 1 & 0 & 0 & 0 & 0 & 0 & 0 & 0 & 0 & 0 & 0 & 0 \\ 0 & 0 & 0 & -1 & 1 & 0 & 0 & 0 & 0 & 0 & 0 & 0 & 0 & 0 & 0 \\ 0 & -1 & 0 & 0 & -1 & 1 & 0 & 0 & 1 & 0 & 0 & 0 & 0 & 0 & 0 \\ 0 & 0 & 0 & 0 & 0 & -1 & 1 & 0 & 0 & 0 & 0 & 0 & 0 & 0 & 0 \\ 0 & 0 & 0 & 0 & 0 & 0 & -1 & 1 & 0 & 0 & 0 & 0 & 0 & 0 & 0 \\ 0 & 0 & 0 & 0 & 0 & 0 & 0 & 0 & -1 & 1 & 0 & 0 & 0 & 0 & 0 \\ 0 & 0 & 0 & 0 & 0 & 0 & 0 & 0 & 0 & -1 & 1 & 0 & 0 & 0 & 0 \\ 0 & 0 & 0 & 0 & 0 & 0 & 0 & 0 & -1 & 0 & 0 & -1 & -1 & -1 & -1 \end{bmatrix} \end{array} \quad (17)$$

$$Q_{[9x15]} = \begin{array}{c} \\ Cut1 \\ Cut\ 2 \\ Cut\ 3 \\ Cut\ 4 \\ Cut\ 5 \\ Cut\ 6 \\ Cut\ 7 \\ Cut\ 8 \\ Cut\ 9 \end{array} \begin{array}{c} \begin{array}{ccccccccccccccc} 1 & 2 & 3 & 4 & 5 & 6 & 7 & 8 & 9 & 10 & 11 & m_1a_y & w_1 & m_2a_y & w_2 \end{array} \\ \begin{bmatrix} 1 & 0 & 0 & 0 & 1 & 0 & 0 & 0 & 0 & 0 & 0 & 1 & 1 & 1 & 1 \\ 0 & 1 & 0 & 0 & 1 & 0 & 0 & 0 & 0 & 0 & 0 & 1 & 1 & 1 & 1 \\ 0 & 0 & 1 & 0 & -1 & 0 & 0 & 0 & 0 & 0 & 0 & 0 & 0 & 0 & 0 \\ 0 & 0 & 0 & 1 & -1 & 0 & 0 & 0 & 0 & 0 & 0 & 0 & 0 & 0 & 0 \\ 0 & 0 & 0 & 0 & 0 & 1 & 0 & 0 & 0 & 0 & 0 & 1 & 1 & 1 & 1 \\ 0 & 0 & 0 & 0 & 0 & 0 & 1 & 0 & 0 & 0 & 0 & 1 & 1 & 1 & 1 \\ 0 & 0 & 0 & 0 & 0 & 0 & 0 & 1 & 0 & 0 & 0 & 1 & 1 & 1 & 1 \\ 0 & 0 & 0 & 0 & 0 & 0 & 0 & 0 & 1 & 0 & -1 & 0 & 0 & 0 & 0 \\ 0 & 0 & 0 & 0 & 0 & 0 & 0 & 0 & 0 & 1 & -1 & 0 & 0 & 0 & 0 \end{bmatrix} \end{array} \quad (18)$$

$$Q_{[9x15]} = \begin{array}{c} \\ Cut1 \\ Cut\ 2 \\ Cut\ 3 \\ Cut\ 4 \\ Cut\ 5 \\ Cut\ 6 \\ Cut\ 7 \\ Cut\ 8 \\ Cut\ 9 \end{array} \begin{array}{c} \begin{array}{ccccccccccccccc} 1 & 2 & 3 & 4 & 6 & 7 & 8 & 9 & 10 & 5 & 11 & m_1a_y & w_1 & m_2a_y & w_2 \end{array} \\ \begin{bmatrix} 1 & 0 & 0 & 0 & 0 & 0 & 0 & 0 & 0 & 1 & 0 & 1 & 1 & 1 & 1 \\ 0 & 1 & 0 & 0 & 0 & 0 & 0 & 0 & 0 & 1 & 0 & 1 & 1 & 1 & 1 \\ 0 & 0 & 1 & 0 & 0 & 0 & 0 & 0 & 0 & -1 & 0 & 0 & 0 & 0 & 0 \\ 0 & 0 & 0 & 1 & 0 & 0 & 0 & 0 & 0 & -1 & 0 & 0 & 0 & 0 & 0 \\ 0 & 0 & 0 & 0 & 1 & 0 & 0 & 0 & 0 & 0 & 1 & 1 & 1 & 1 & 1 \\ 0 & 0 & 0 & 0 & 0 & 1 & 0 & 0 & 0 & 0 & 1 & 1 & 1 & 1 & 1 \\ 0 & 0 & 0 & 0 & 0 & 0 & 1 & 0 & 0 & 0 & 1 & 1 & 1 & 1 & 1 \\ 0 & 0 & 0 & 0 & 0 & 0 & 0 & 1 & 0 & 0 & -1 & 0 & 0 & 0 & 0 \\ 0 & 0 & 0 & 0 & 0 & 0 & 0 & 0 & 1 & 0 & -1 & 0 & 0 & 0 & 0 \end{bmatrix} \end{array} \quad (19)$$

$$Q_{[9x31]} = \begin{array}{c} \\ Cut1 \\ Cut\ 2 \\ Cut\ 3 \\ Cut\ 4 \\ Cut\ 5 \\ Cut\ 6 \\ Cut\ 7 \\ Cut\ 8 \\ Cut\ 9 \end{array} \begin{array}{c} \begin{array}{ccccccccccccccc} F_{y1} & F_{z1} & M_{x2} & F_{p2} & F_{LS2} & \cdots & M_{x5} & F_{p5} & F_{LS5} & F_{y11} & F_{z11} & m_1a_y & w_1 & m_2a_y & w_2 \end{array} \\ \begin{bmatrix} 1 & 1 & 0 & 0 & 0 & \cdots & 1 & 1 & 1 & 0 & 0 & 1 & 1 & 1 & 1 \\ 0 & 0 & 1 & 1 & 1 & \cdots & 1 & 1 & 1 & 0 & 0 & 1 & 1 & 1 & 1 \\ 0 & 0 & 0 & 0 & 0 & \cdots & -1 & -1 & -1 & 0 & 0 & 0 & 0 & 0 & 0 \\ 0 & 0 & 0 & 0 & 0 & \cdots & -1 & -1 & -1 & 0 & 0 & 0 & 0 & 0 & 0 \\ 0 & 0 & 0 & 0 & 0 & \cdots & 0 & 0 & 0 & 1 & 1 & 1 & 1 & 1 & 1 \\ 0 & 0 & 0 & 0 & 0 & \cdots & 0 & 0 & 0 & 1 & 1 & 1 & 1 & 1 & 1 \\ 0 & 0 & 0 & 0 & 0 & \cdots & 0 & 0 & 0 & 1 & 1 & 1 & 1 & 1 & 1 \\ 0 & 0 & 0 & 0 & 0 & \cdots & 0 & 0 & 0 & -1 & -1 & 0 & 0 & 0 & 0 \\ 0 & 0 & 0 & 0 & 0 & \cdots & 0 & 0 & 0 & -1 & -1 & 0 & 0 & 0 & 0 \end{bmatrix} \end{array} \quad (20)$$

Taking into consideration that each joint has constraints (Table 3), this is what allows the cut-set matrix's extent (Eq. 19), as shown in Fig. 10 and Eq. 20.

Equation system solutions

Using the cut-set law [12], the algebraic sum of the normalized wrenches that belong to the same cut (Eq. 20) must be equal to zero; this allows to structure the mechanism's static matrix (Eq. 21) or the mechanism's extended matrix of the (Eq. 22).

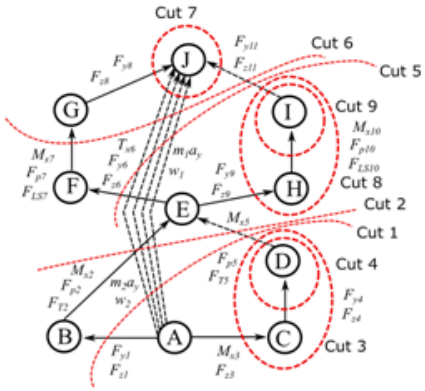

Figure 10: Extended cut-set action graph

$$\left[\hat{A}_n\right]_{27\times31}.[\Psi]^T_{1\times31} = [0]_{27\times1} \quad (21)$$

In Eq 22, it is essential to identify the set of primary variables ($[\hat{A}_{ns}]$) (w_1, m_1a_y, w_2, m_2a_y) as well as the secondary variables ($[\hat{A}_{np}]$), which must be reorganized placing the important variables for the calculation of the mechanism's stability on it's backside, such as the tires' supporting forces (F_{z1}, F_{z3}), the tires' normal forces (F_{T2} y F_{T5}) and the leaf springs' normal forces (F_{LS7} y F_{LS10}), as shown in Eq. 23. By solving the Eq. 23 using the Gauss-Jordan method, all secondary variables are expressed in terms of the primary variables, with them, the equation to determine the support force of the inner tire while taking a curve stand out (F_{z3}) (Eq. 24).

$$\begin{array}{c} \\ Cut\ 1 \\ \\ \\ Cut\ 2 \\ \\ \vdots \\ \\ Cut\ 9 \end{array} \begin{array}{c} \begin{bmatrix} 0 & 0 & 0 & 0 & 0 & \cdots & 0 & h_1 & tb_1 & h_2 & tb_2 \\ 1 & 0 & 0 & 0 & 0 & \cdots & 0 & -1 & 0 & -1 & 0 \\ 0 & 1 & 0 & 0 & 0 & \cdots & 0 & 0 & -1 & 0 & -1 \\ 0 & 0 & 1 & -l_1 & 0 & \cdots & 0 & h_1 & tb_1 & h_2 & tb_2 \\ 0 & 0 & 0 & c1 & 0 & \cdots & 0 & -1 & 0 & -1 & 0 \\ 0 & 0 & 0 & s1 & 0 & \cdots & 0 & 0 & -1 & 0 & -1 \\ \vdots & \vdots & \vdots & \vdots & \vdots & \vdots & \vdots & \vdots & \vdots & \vdots & \vdots \\ 0 & 0 & 0 & 0 & 0 & \cdots & -p_{14} & 0 & 0 & 0 & 0 \\ 0 & 0 & 0 & 0 & 0 & \cdots & 0 & 0 & 0 & 0 & 0 \\ 0 & 0 & 0 & 0 & 0 & \cdots & -1 & 0 & 0 & 0 & 0 \end{bmatrix}_{27\times31} \end{array} \begin{bmatrix} F_{y1} \\ F_{z1} \\ M_{x2} \\ F_{p2} \\ F_{LS2} \\ \vdots \\ F_{z11} \\ m_1a_y \\ w_1 \\ m_2a_y \\ w_2 \end{bmatrix}_{31\times1} = [0]_{27\times1} \quad (22)$$

$$\left[\hat{A}_{ns}\right]_{27\times27}.[\Psi_s]^T_{1\times27} + \left[\hat{A}_{np}\right]_{27\times4}.[\Psi_p]^T_{1\times4} = [0]_{27\times1} \quad (23)$$

$$F_{z3} + \left(\frac{h_1}{t}\right)m_1a_y - \left(\frac{tb_1}{t}\right)m_1g + \left(\frac{h_2}{t}\right)m_2a_y - \left(\frac{tb_2}{t}\right)m_2g = 0 \quad (24)$$

Taking into account that at the rollover limit, this force (F_{z3}) tends to zero, the Static Rollover Threshold (SRT) is calculated using:

$$SRT = \frac{a_y}{g} = \frac{tb_1m_1 + tb_2m_2}{h_1m_1 + h_2m_2} \quad (25)$$

This equation tells us that the stability factor does not only depend on the position of the centers of gravity, but also depends on the fixed weight of the vehicle and the weight of the liquid transported.

CASE STUDY

For this study, we used the model of a tanker truck (Figure 2) with the following specifications:

Table 4: Vehicle characteristics

Road tanker		
Parameter	Valor	Unidad
Weight of empty vehicle (w_1)	60	kN
Weight of transported liquid (w_2) - (water)	407.66	kN
Combined stiffness of suspension - (3 axles)	5400	kN/m
Combined stiffness of tires	5040	kN/m
Side distance between the wheels or track width (t)	1.86	m
Tank diameter	1.015	m
CG1 initial height (h_1)	0.85	m
Initial height of the tanks geometric center	2.125	m
Lateral separation distance of the suspension (b)	0.95	m

For the stability factor's calculation, ISO-14792 - Steady State Circular Test [14] was taken into account and for road safety the lateral load transfer must not be greater than 60% [15], [16], once the model was implemented, the centripetal forces (m1ay and m2ay) were gradually increased until the lateral load transfer was the recommended one. In Figure 11 it can be seen how initially the stability of the vehicle is quite high, but as the tank is filled and the weight of the liquid (w2) increases, the stability factor decreases since the height of its center of gravity (h2) is gradually increasing. Additionally, it can be observed how the vehicle's inclination angle increases with more filling on the tank due to the action suspension tires stiffness (Body roll angle - θ). Moreover, in Figure 11 it can be evidenced how the fluid's movement decreases the vehicle's stability factor since it is not allowed to move the fluid. As can be seen from Figs. 12 and 13 the stability is mostly affected for tank filling levels between 40% and 60%, meaning an average reduction of the stability factor of 0:01356. From Eq. 25, and as indicated in Eq. 26, it is known that the stability factor can be expressed as a function of vehicle velocity (V) when taking a curve and taking into consideration the radius of the curve (R), therefore, for a vehicle with fluid movement and without fluid movement, and with a tank filling level of 50%, in a curve of R = 100 m a speed reduction of approximately 2.4km/h can be evidenced, this is really important to detail since it allows to point out the need to develop mechanisms that prevent lateral fluid movement of the, type breakwater, which would increase vehicle stability and road safety.

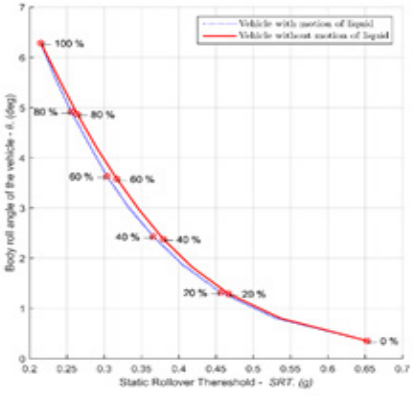

Figure 11: SRT behaviour

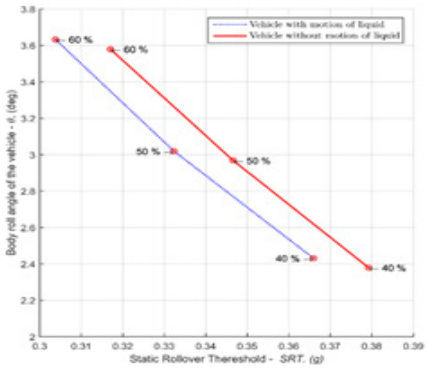

Figure 12: SRT behaviour (40% - 60%)

$$SRT = \frac{a_y}{g} = \frac{V^2}{R\,g} \tag{26}$$

CONCLUSIONS

In this paper, the stability factor for tanker truck type vehicles was determined. In it, it can be evidenced that this factor is not only a function of the vehicle's center of gravity location, but it is also a function of the vehicle's fixed and mobile weight. In the results of the test performed, it was possible to show that as the vehicle acquires a greater load, the stability decreases, this is due to the fact that the height (h2) of the vehicle's liquid weight center of gravity increases. Additionally, it was determined that the stability of the vehicles can be increased if mechanisms that prevent the lateral movement of the transported fluid are developed. This development will be proposed for future circular section tanker truck research, and other types of the aforementioned.

REFERENCES

1. Rajagounder, R., Mohanasundaram, G. V., Kalakkath, P. (2016). A study of liquid sloshing in an automotive fuel tank under uniform acceleration. Engineering Journal, vol. 20, no. 1, 71-85, DOI: 10.4186/ej.2016.20.1.71

2. Ranganathan, R. (1993). Rollover threshold of partially filled tank vehicles with arbitrary tank geometry. Proceedings of the Institution of Mechanical Engineers, Part D: Journal of Automobile Engineering, vol. 207, no. 3, 241-244, DOI: 10.1243/PIME_PROC_1993_207_185_02
3. Dasgupta, A. (2011). Effect of tank cross-section and longitudinal baffles on transient liquid slosh in partly-filled road tankers. Doctoral dissertation, Concordia University.
4. Winkler, C. (2000). Rollover of Heavy Commercial Vehicles. UMTRI Research Review, The University of Michigan Transportation Research Institute, v. 31, n. 4, p. 120.
5. Billing, J. R., Patten, J. D. (2005). An assessment of tank truck roll stability. Report TP, 14237.
6. Prem, H., Mai, L., Brusza, L. (2006). Tilt testing of two heavy vehicles and related performance issues. In International Symposium on Heavy Vehicle Weights and Dimensions, 9th.
7. Moreno, G., Nicolazzi, L. C., Vieira, R. D. S., Martins, D. (2017). Suspension and tyres: stability of heavy vehicles. International Journal of Heavy Vehicle Systems, vol. 24, no. 4, 305-326, DOI: 10.1504/IJHVS.2017.087221
8. Davies, T. H. (1983). Mechanical networks-III wrenches on circuit screws. Mechanism and Machine Theory, vol. 18, no. 2, 107112.
9. Moreno, G. G., Peña, C. A., Gualdron, O. E. (2020). Stress Analysis of a Landing Gear Using the Davies Method. Periodica Polytechnica Mechanical Engineering, vol. 64, no. 3, 256-262. DOI: 10.3311/PPme.16392
10. Cengel Yunus, A., Cimbala John, M. (2006). Fluid Mechanics Fundamentals and Applications. Editorial McGrawHill.
11. Davies, T. H. (1983). Mechanical networks-III wrenches on circuit screws. Mechanism and Machine Theory, vol. 18, no. 2, p. 107112.
12. Davies, T. H. (2000). The 1887 committee meets again. Subject: freedom andconstraint. Ball 2000 Conference, Cambridge University Press, Trinity College, Cambridge, UK., p. 56.
13. Tsai, L. W. (1999). Robot Analysis - The Mechanism of Serial and Paralle Manipulators. New York: John Wiley & Sons. ISBN 0-471-32593-7.
14. ISO-14792. (2011). Heavy commercial vehicles and buses – Steady state circular tests. International Organization for Starndardization. Geneva, Switzerland.
15. Woodrooffe, J., Sweatman, P., Arbor, A., Middleton, D., James, R., Billing, J. R. (2010). National Cooperative Highway Research Program NCHRP. Report 671. Review of Canadian Experience with the Regulation of Large Commercial Motor Vehicles. Ed. National Academy of Sciences, Washington, D.C., ISBN 978-0-309-15518-2.
16. Walker, H. K., Pearson, J. R. (1987). Recommended regulatory principles for interprovincial heavy vehicle weights and dimensions. Tech. rep., CCMTA/RTAC Vehicle Weights and Dimensions Study Implementation Committee Report.

Paper submitted: 14.08.2021.
Paper accepted: 06.11.2021.